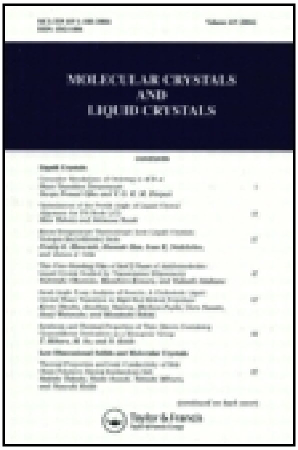

Molecular Crystals and Liquid Crystals
Publication details, including instructions for authors and subscription information:
http://www.tandfonline.com/loi/gmcl20

Phase Transitions and Physical Properties of a Binary Mixture of Bicyclohexane Compounds, II: X-ray Diffraction Measurements

Malay Kumar Das [a] , Prithwi Dev Roy [a] , Sukla Paul [a] , Ranjit Paul [a] & Banani Das [b]
[a] Department of Physics, North Bengal University, Siliguri, India
[b] Department of Physics, Siliguri Institute of Technology, Siliguri, India

Version of record first published: 31 Jan 2007

To cite this article: Malay Kumar Das, Prithwi Dev Roy, Sukla Paul, Ranjit Paul & Banani Das (2006): Phase Transitions and Physical Properties of a Binary Mixture of Bicyclohexane Compounds, II: X-ray Diffraction Measurements, Molecular Crystals and Liquid Crystals, 457:1, 55-66

To link to this article: http://dx.doi.org/10.1080/15421400500447140

Mol. Cryst. Liq. Cryst., Vol. 457, pp. 55–66, 2006
Copyright © Taylor & Francis Group, LLC
ISSN: 1542-1406 print/1563-5287 online
DOI: 10.1080/15421400500447140

Phase Transitions and Physical Properties of a Binary Mixture of Bicyclohexane Compounds, II: X-ray Diffraction Measurements

Malay Kumar Das
Prithwi Dev Roy
Sukla Paul
Ranjit Paul
Department of Physics, North Bengal University, Siliguri, India

Banani Das
Department of Physics, Siliguri Institute of Technology, Siliguri, India

X-ray diffraction data from a binary mixture of two isomeric nonpolar bicyclohexane compounds containing alkenyl side chains have been analyzed to determine the bond orientational order (BOO), orientational order parameters (OOP), layer thickness (in Smectic B phase), apparent molecular length (in nematic phase), and lateral molecular distance, D, as a function of temperature. The phase diagram shows the presence of a two-phase smectic B–nematic co-existing region. The orientational order parameter (OOP) values drop sharply with an increase in temperature within the co-existing phase, which is because the observed OOP value is the weighted mean OOP of the two phases. Interestingly, the BOO values are found to increase with an increase in temperature in the co-existing smectic, B–nematic phase. The transverse correlation lengths in the smectic, co-existing, and nematic phases have also been estimated. These values are found to diverge as the co-existing smectic B–nematic phase region is approached, indicating a second-order phase transition. This result has also been supported by entropy, density, refractive index, and OOP measurements.

Keywords: bicyclohexane; binary mixture; bond orientational order; co-existing phase; correlation length; orientational order parameter

INTRODUCTION

In our earlier paper [1], we reported the phase diagram, Differential Scanning Calorimetry (DSC), refractive indices, and density measurements

Address correspondence to Malay Kumar Das, Department of Physics, North Bengal University, Siliguri, India. E-mail: mkdnbu@yahoo.com

of a binary mixture of two isomeric nonpolar bicyclohexane compounds containing alkeny1 side chains. The compounds, one only a nematic (N) phase (1d(3)CCO_2) and the other only a smectic B (SmB) phase (0d(4)CCO_2), are characterized by similar molecular structures, except for a shift in the position of a double bond [2]. In this article, we report the results of x-ray diffraction measurements done on a few selected compositions of this mixture that show both the SmB and N phases. One of the most interesting feature of these mixtures is the presence of a two-phase SmB–N co-existing region over a temperature range of about 2.5–3°C. Two mixtures with molar concentrations of 1d(3)$CCO_2 = 0.6$ (mixture A) and 0.73 (mixture B) have been studied thoroughly throughout the entire mesomorphic range. DSC studies [1] for these two mixtures show a weakly first-order or second-order phase transition in going from the SmB to the N phase.

According to Birgeneau and Lister [3], the SmB phase is a realization of the stacked hexagonal phase possessing the bond orientational order (BOO) found in two dimensions. The order parameter associated with a system having six-fold symmetry, as in the case of SmB liquid crystals, is the BOO, defined to be the thermal average of the quantity

$$\psi(\mathbf{r}) = \langle \exp(i6\theta(\mathbf{r})) \rangle, \tag{1}$$

where the bond angle $\theta(\mathrm{r})$ is the orientation, relative to any fixed laboratory axis, of a bond between two nearest neighbor molecules. The x-ray diffraction patterns have been analyzed to determine the temperature dependence of the BOO in the SmB phase of only mixture A, where it has been possible to obtain a good mono-domain sample.

Orientational order parameters (OOP) have been studied throughout the entire mesomorphic range for mixtures A and B. The intermolecular distance, layer thickness, and apparent molecular lengths in several mixtures [x = 0.3, 0.4, 0.5, 0.6, and 0.73, where x is the molar fraction of (1d(3)CCO_2)] have also been studied. X-ray diffraction measurements of the pure compounds have already been done earlier in our laboratory [4,5]. Although x-ray [6–12] and electron diffraction [13,14] studies on SmB phase have been reported so far, not much work has been done to determine the BOO and OOP in SmB phase of bicyclohexane compounds. The BOO values obtained by us have been utilized to characterize the SmB phase, which is found to be of the crystal B type. The BOO values of mixture A are found to be nearly independent of temperature in the SmB phase but increase with temperature within the co-existing SmB-N phase. The transverse correlation length diverges near the vicinity of the two phase co-existing SmB-N region, indicating a second-order phase transition.

EXPERIMENTAL

X-ray diffraction patterns were recorded on an x-ray film using a flat plate camera at several temperatures within the mesomorphic phase using Ni-filtered CuK_α radiation of wavelength $\lambda = 1.542\,\text{Å}$. For the x-ray diffraction study, the pure compounds as well as their mixtures could not be aligned even in a magnetic field of about 0.6 T. Because the magnetic susceptibility anisotropy, Δ_χ, for these compounds is almost zero, it was not possible to obtain monodomain samples by application of a magnetic field. However, we succeeded in obtaining very good monodomain samples in which the hexagonal symmetry of the SmB phase extended throughout the bulk sample by controlled cooling (at the rate of 0.1 °C/min) of the samples kept in 0.5-mm-diameter glass capillaries, from the isotropic state to room temperature (~20°C). By trial, a monodomain sample was selected and the capillary was rotated in such a way that the layer normal coincided with the direction of the x-ray beam. At this position of the capillary, x-ray diffraction photographs were recorded. Because of a lack of cooling facilities in our laboratory, we could not take photographs below room temperature. Photographs of OOP measurements were taken after rotating the sample-filled capillary 90° with respect to the previous position such that the smectic layers were parallel to the direction of x-ray beam.

The x-ray diffraction photographs were scanned by a Mustek 1200 UB scanner. The gray mode scan was used, and the resolution was set at 600 dpi. Optical densities of the pixels were calculated and then converted to X-ray intensities with the help of a calibration curve following the procedure of Klug and Alexander [15]. Origin 7.0 software was used for data analysis purpose.

The transition temperatures of the pure compounds, their structural formulas, and chemical names are shown in Schemes 1 and 2.

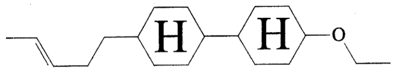

SCHEME 1 Component 1: C $\underset{24.5^\circ C}{\overset{44^\circ C}{\rightleftharpoons}}$ N $\xrightarrow{76.5^\circ C}$ I. 4(3″-Penenyl) 4′(ethoxyl) 1,1′ bicyclohexane ($1d(3)CCO_2$).

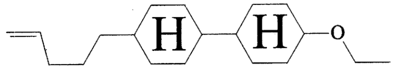

SCHEME 2 Component 2: C $\xrightarrow{11^\circ C}$ Sm B $\xrightarrow{43^\circ C}$ I. 4-Ethoxyl, 4′-pent-4″-enyl bicyclohexane ($0d(4)CCO_2$).

RESULTS AND DISCUSSION

The phase diagram of this system as observed by us is shown in Fig. 1. From the phase diagram, it observed that for mixtures within the concentration range $0.2 < x < 0.8$ (x = molar fraction of 1d(3)CCO_2), both SmB and N phases are present. For mixtures with molar fractions between $x \approx 0.5$ and $x \approx 0.8$, a two-phase (SmB–N) co-existing region is observed (~2.5–3°C). The phase could be identified distinctly under the polarizing microscope, and the co-existing phases are quite stable. All the mixtures show large supercooling. Although the melting temperatures of the mixtures vary linearly with concentration, the clearing temperatures deviate significantly from linearity, with the depression being highest near $x \approx 0.4$.

Figure 2a shows the x-ray diffraction photograph of the aligned sample in the SmB phase of mixture A at 25°C where the incident x-ray beam is parallel to the layer normal. The outer diffraction ring is split up into six spots, clearly showing the hexagonal molecular arrangement within the layers. Almost identical photographs have been observed from room temperature up to the SmB to N phase

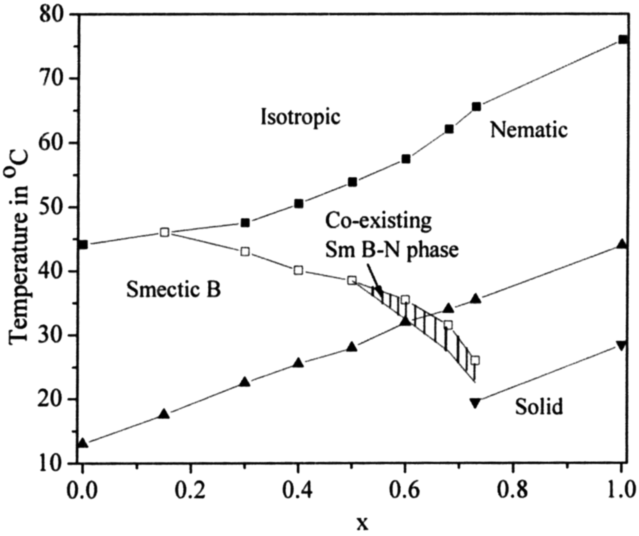

FIGURE 1 Temperature-concentration phase diagram for the binary system of 1d(3)CCO_2 and 0d(4)CCO_2. The mole fraction of 1d(3)CCO_2 is x. ■ nematic (smectic B)–isotropic transition temperature, □ smectic B–nematic transition temperature, ▲ melting temperature, and ▼ the temperature to which the sample could be supercooled without solidification. The shaded region represents the co-existing smectic B–nematic phase.

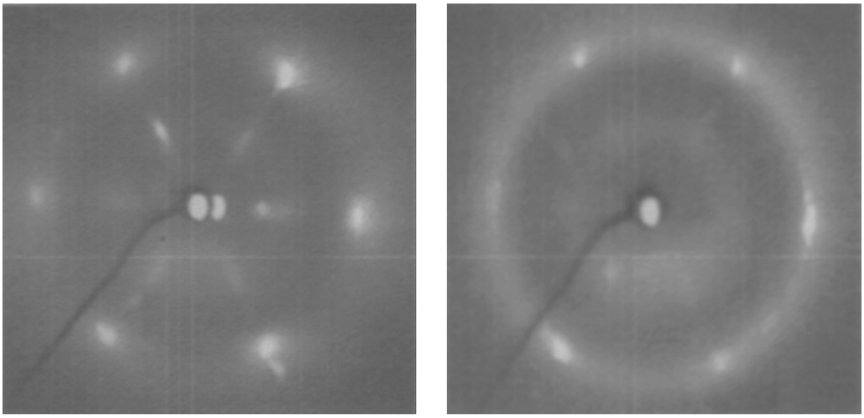

FIGURE 2 X-ray diffraction photograph from an aligned sample of mixture A ($x = 0.6001$), where the incident x-ray beam is parallel to the layer normal: (a) smectic B phase at 25°C, and (b) co-existing smectic B–nematic phase at 35.5°C.

transition except in the co-existing SmB-N phase. The co-existing phase is marked by the appearance of relatively sharp x-ray diffraction spots exhibiting the hexagonal symmetry of the SmB phase, superimposed on the diffuse liquid-like outer ring characteristics of the N phase with the direction of the incident beam parallel to the N director (Fig. 2b), indicating the presence of both N and SmB domains. Similar behavior of these mixtures has been observed from refractive index measurements made by us [1], where we have been able to observe and measure the refractive indices for both the SmB and N phase in the co-existing region.

The x-ray diffraction pattern of a well-oriented monodomain sample of mixture A in the SmB-N co-existing phase and N phases are shown in Figs. 3a–b, respectively. These photographs are obtained after slow cooling of a drop of the liquid crystal placed on a glass plate with the x-ray beam incident parallel to the glass plate. The x-ray patterns are recorded using a two-dimensional (2-D) area detector (HI–Star, Siemens AG).

The BOO has been calculated by evaluating the expression

$$\langle \cos(6\theta) \rangle = \frac{\int_0^{\pi/6} \cos(6\theta) f(\theta) d\theta}{\int_0^{\pi/6} f(\theta) d\theta}, \qquad (2)$$

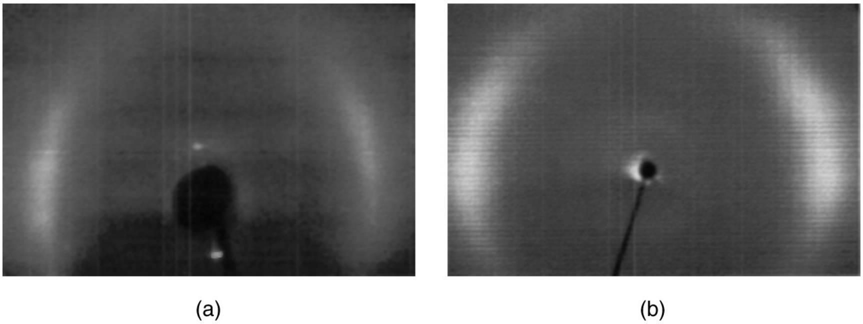
(a) (b)

FIGURE 3 X-ray diffraction pattern of an aligned sample of mixture A, where the x-ray beam is incident perpendicular to the layer normal: (a) smectic B–nematic co-existing phase at 35°C, and (b) nematic phase at 38°C.

where f(θ) is the angular distribution function of center of mass of the neighboring molecules with respect to a central molecule, and the angular distribution function has a maximum at $\theta = 0$. This equation can be approximated by the following expression:

$$\langle\cos(6\theta)\rangle \approx \frac{\int_0^{\pi/6}\cos(6\theta)\mathrm{I}(\theta)\mathrm{d}\theta}{\int_0^{\pi/6}\mathrm{I}(\theta)\mathrm{d}\theta}, \tag{3}$$

where I(θ) is the azimuthal distribution of the x-ray diffraction intensity. According to Vainshtein [16] it has been assumed that I(θ), the intensity distribution, is proportional to f(θ), the distribution function, and consequently has its maximum at $\theta = 0$. BOO is calculated for each peak, and finally the average over six peaks is taken. The intensity values plotted against azimuthal angular positions have been corrected for the background (scattered) intensity values. Figure 4 shows the BOO values at different temperatures in the SmB phase for mixture A. The BOO in the SmB phase of this mixture is found to be $\sim$0.96 and independent of temperature throughout the SmB phase. This result seems to indicate that the SmB phase for this mixture is of the crystal B type in the sense that the molecular positions exhibit long-range BOO throughout the phase. Interestingly, BOO values increase rapidly with temperature in the co-existing SmB-N phase. This increase may be due to the pretransitional effect of the SmB-N second-order phase transition.

The transverse correlation length in the SmB as well as in the N phase of mixtures A and B has been determined from a linear scan of the x-ray diffraction peaks. X-ray intensities were at first corrected for the use of a flat-plate camera. This corrected intensity data was

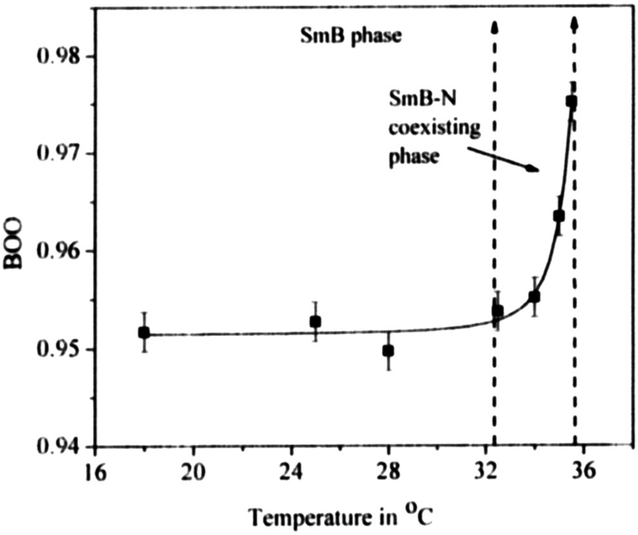

FIGURE 4 Temperature dependence of bond orientational order (BOO) for mixture A. The vertical bars indicate estimated errors. The solid line is a guide to the eye only.

then deconvoluted for finite width of the collimator. The deconvoluted intensity profile I(q) was fitted to a Lorentzian form with a quadratic background, namely,

$$I(q) = \frac{a_1}{a_2 + (q - q_o)^2} + a_3 q^2 + a_4 q + a_5, \tag{4}$$

with q being the magnitude of the scattering vector. The transverse correlation length is defined as $\xi = 2\pi(a_2)^{-1/2}$. The in-plane transverse resolution Δq for this instrument is $6 \times 10^{-3}\,\text{Å}^{-1}$. The values of the correlation lengths obtained varied from 35 Å to 50 Å in SmB phase and 18 Å to 25 Å in N phase for these mixtures. For crystal B phase, the correlation lengths are expected to be much longer. One reason for this discrepancy may be due to the use of Ni-filtered Cu K_α radiation, which contains a white background radiation in addition to the Cu K_α peak. No correction for this white radiation, which broadens the diffraction peaks considerably, is made here. Hence, the experimental values of correlation lengths as obtained previously are much shorter than the theoretically expected values. Figure 5 shows the measurements of transverse correlation length over the entire mesomorphic temperature region for mixture A. These values are found to diverge as the co-existing phase region is approached from either

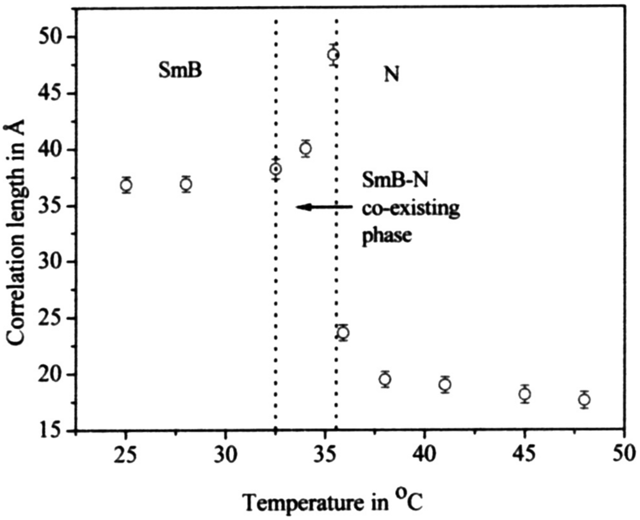

FIGURE 5 Temperature dependence of the transverse correlation length for mixture A. The vertical bars indicate estimated errors.

side, indicating a second-order phase transition. This has been supported by entropy, density, refractive index, and OOP measurements [1]. The temperature variation of transverse correlation length for mixture B also shows a similar trend.

The angular distribution of the x-ray diffraction intensities for mixtures A and B are used to measure the orientational distribution function $f(\theta)$ and hence the OOP $\langle P_2 \rangle$ throughout their entire mesomorphic range following a procedure reported earlier [17]. Figures 6 and 7 show the variation of the experimentally determined OOPs with temperature for the two mixtures A and B respectively. The experimental $\langle P_2 \rangle$ values are relatively high in the SmB phase, showing the phase to be much more orientationally ordered than its neighboring N phase. In the coexisting SmB-N phase, a very sharp decrease of the OOP values is observed with increase in temperature. This OOP is in effect the weighted mean OOP of the two phases. This is due to the fact that in this two-phase region, the SmB domains rapidly reduce in size with increasing temperature, so that the weighted mean OOP decreases rather rapidly. Similar results are also observed in the OOP values obtained from the refractive index measurements, which are also included in the respective figures.

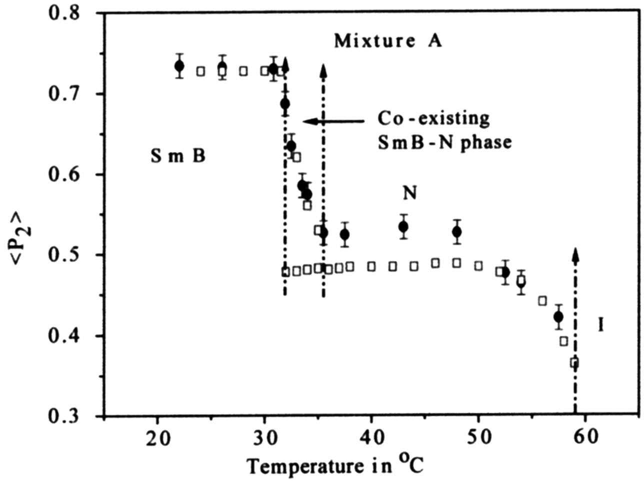

FIGURE 6 Temperature dependence of $\langle P_2 \rangle$ values for mixture A: □ $\langle P_2 \rangle$ from refractive index data, and • $\langle P_2 \rangle$ from x-ray data. The vertical bars indicate estimated errors.

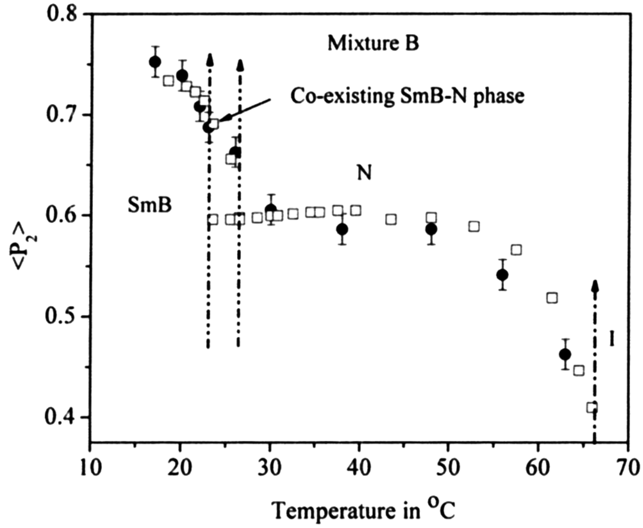

FIGURE 7 Temperature dependence of $\langle P_2 \rangle$ values for mixture B: □ $\langle P_2 \rangle$ from refractive index data, and • $\langle P_2 \rangle$ from x-ray data. The vertical bars indicate estimated errors.

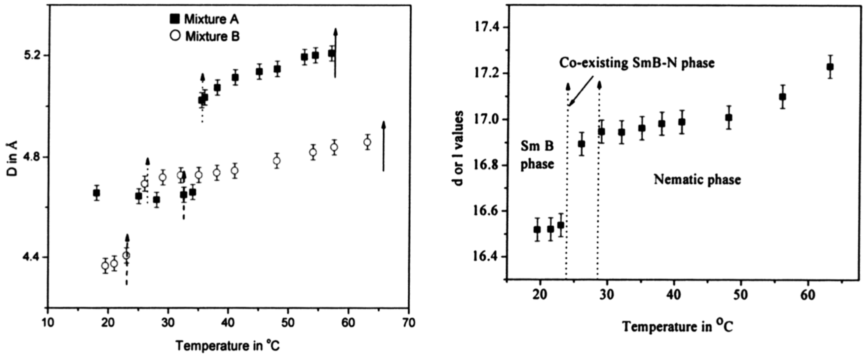

(a) (b)

FIGURE 8 (a) Temperature dependence of D values for mixture A and B: ■ MixA, ○ MixB; ↑ for nematic to isotropic transition; ↑ for co-existing SmB-N to nematic transition; and ↑ for SmB to SmB–N coexisting transition. The vertical bars indicate estimated errors; (b) Temperature dependence of d values for mixture B. The vertical bars indicate estimated errors.

The values of the apparent molecular length or layer thickness (d) and the intermolecular distance D at different temperatures are also measured for mixtures with $x = 0.3,\ 0.4,\ 0.5,\ 0.6,$ and 0.73. The temperature variation of the intermolecular distance, D, for mixtures A and B throughout the mesomorphic range are shown in Fig. 8a. There is an increase in the D values from the SmB to N phase transition. This increase is most sharp at the transition to the co-existing phase, and these values also continue to increase within this phase. The reason for this is the same as stated for the variation of OOP in the two-phase region. As observed from Fig. 8a, the variation of D with temperature in the N phase is quite appreciable, caused by the increasing thermal vibrations of the chain parts of these flexible molecules. As expected, the temperature variation of d in the smectic phase is slight. However, for all the mixtures, the apparent molecular lengths (l) increase with increasing temperature, and the effect is pronounced near the N-I phase transition (Fig. 8b). This increase before the phase transition is once again due to the increasing thermal variations of the chain parts just before the transition. The d values in the SmB phase are more or less the same for all the mixtures (Fig. 9) and are almost equal to the respective model molecular lengths of the isomeric pure components. However, the D values in the SmB phase decreases with the increase in molar fraction of 1d(3)CCO$_2$. At a temperature $T = T_{NI} - 2.5°C$, in the N phase of this system, the D values show an enhancement in their magnitudes

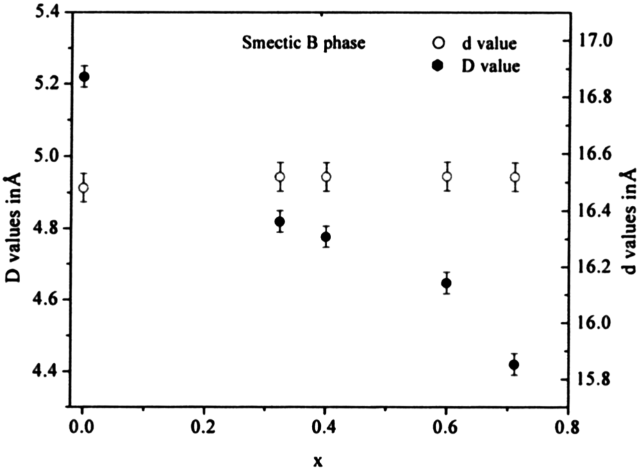

FIGURE 9 Variation of layer spacing (d) and intermolecular distance (D) with molar fraction (x) of 1d(3)CCO_2 in the smectic phase: o d values, and • D values. The vertical bars indicate estimated errors.

near $x \approx 0.6$ (Fig. 10). This implies the packing of the molecules in the nematic phase is poor near this region. The l values in the N phase, however, slightly increase with increase in the molar fraction of 1d(3)CCO_2.

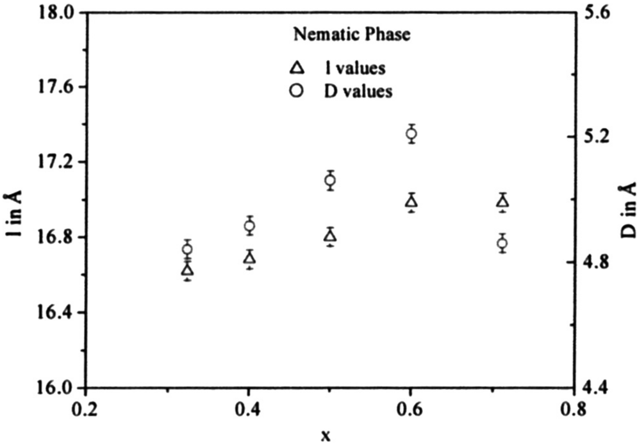

FIGURE 10 Variation of apparent molecular length (l) and intermolecular distance (D) with molar fraction (x) of 1d(3)CCO_2 in the nematic phase at $T = T_{NI} - 2.5°C$: Δ 1 values, and o D values. The vertical bars indicate estimated errors.

ACKNOWLEDGMENTS

The authors are thankful to S. Diele, Institute for Physical Chemistry, Martin Luther University, Halle, Germany, for fruitful discussions. We extend our gratitude to him for kindly allowing us to record the x-ray diffraction patterns for mixtures A and B on the 2-D area detector during one of the authors' (M. K. D) stay in Halle. We are also grateful to M/S Hoffmann-La-Roche and Co., Basel, Switzerland, for kindly donating the liquid-crystalline samples used in this work. One of the authors (B. D.) is thankful to the Council of Scientific and Industrial Research, New Delhi, India, for the award of a research associateship.

REFERENCES

[1] Dev Roy, P., Das, M. K., Paul, S., Paul, R., & Das, B. (2006). *Mol. Cryst. Liq. Cryst.*, *457*, 43.
[2] Schadt, M., Buchecker, R., & Müller, K. (1989). *Liq. Cryst.*, *5*, 293.
[3] Birgeneau, R. J. & Lister, J. D. (1978). *J. Phys. Lett.*, *39*, L-399.
[4] Nath, A., Chaudhury, B., & Paul, S. (1995). *Mol. Cryst. Liq. Cryst.*, *265*, 699.
[5] Adhikari, B. & Paul, R. (1996). *Phase Transitions*, *56*, 165.
[6] Haung, C. C., & Stoebe, T. (1993). *Adv. Phys.*, *42*, 343.
[7] Brownsey, G. J. & Leadbetter, A. J. (1980). *Phys. Rev. Lett.*, *44*, 1608.
[8] Gane, P. A. C. & Leadbetter, A. J. (1983). *J. Phys. C.: Solid State Phys.*, *16*, 2059.
[9] Lobo, C. V., Krishna Prasad, S., & Shankar Rao, D. S. (2004). *Phy. Rev. E*, *69*, 051706.
[10] Moncton, D. E. & Pindak, R. (1979). *Phy. Rev. Lett.*, *43*, 701.
[11] Haung, C. C. & Strandburg, K. J. (Eds.), (1992). *Bond Orientational Order in Condensed Matter Systems*, Springer-Verlag: Berlin, p. 78.
[12] Doucet, J., Levelut, A. M., & Lambert, M. (1978). *Ann. Phys.*, *3*, 157.
[13] Kim, A. J., Veum, M., Stoebe, T., Chou, C. F., Ho, J. T., Hui, S. W., Surendranath, V., & Haung, C. C. (1995). *Phy. Rev. Lett.*, *74*(24), 4863.
[14] Cheng, M., Ho, J. H., Hui, S. W., & Pindak, R. (1987). *Phys. Rev. Lett.*, *59*, 1112.
[15] Klug, H. P. & Alexander, L. E. (1974). *X-ray Diffraction Procedure for Polycrystalline and Amorphous Materials*, John Wiley and Sons: New York, pp. 114, 473.
[16] Vainshtein, B. K. (1966). *Diffraction of X-rays by Chain Molecules*, Elsevier: London.
[17] Bhatterjee, B., Paul, S., & Paul, R. (1981). *Mol. Phys.*, *44*, 1391.